Enhanced performance of single and double junction plastic solar cells

Moet, Date Jan David

Chapter 4

Hybrid polymer solar cells with ZnO from diethylzinc

Abstract

Metal oxides can be used as electron acceptor in hybrid organic-inorganic bulk heterojunction solar cells, thus providing an interesting alternative to the fullerene derivatives that we have seen in the previous chapters. Within this class of inorganic materials, zinc oxide is possibly one of the more versatile. When used as an electron acceptor, it can be incorporated in the form of nanoparticles or via in situ conversion of an organozinc precursor. In this chapter, we investigate the effects of the use of diethylzinc as a molecular precursor for zinc oxide in polymer solar cells. We find that upon addition of diethylzinc, the absorption spectrum of MDMO-PPV shifts to the blue and hole transport through the polymer deteriorates dramatically. This indicates a reduction of the conjugation length of the polymer backbone, most probably caused by the breaking of trans vinyl bonds. To prevent such polymer degradation, P3HT is introduced as the electron donor. The system of P3HT and precursor ZnO reveals an unchanged UV-VIS absorption profile and zero-field hole mobility with respect to the pristine polymer, as well as an improved photovoltaic performance with an estimated power conversion efficiency of 1.4%.

Published as:
D. J. D. Moet, L. J. A. Koster, B. de Boer, and P. W. M. Blom, Chem. Mater. **19**, 5856 (2007).

4.1 Introduction

Today's most efficient polymer-based solar cells are constructed from an interpenetrating network of an electron donating polymer and an electron-accepting fullerene derivative.[1] However, other classes of materials with varying optoelectronic properties have been used as an electron acceptor in BHJ solar cells as well, such as *n*-type conjugated polymers[2,3] and inorganic semiconducting materials. The latter is perhaps the most versatile group: mixtures of polymers with nanoparticles of TiO_2[4] and ZnO,[5–7] ZnO nanorods,[8] CdSe nanorods[9] and tetrapods,[10,11] as well as polymers permeated in mesoporous networks of TiO_2[12,13] have been successfully integrated in devices showing a photovoltaic effect.

Another method of realizing a hybrid nanoscale heterojunction consists in adding to the polymer solution a molecular precursor that, via hydrolysis and condensation reactions, converts to the desired *n*-type metal oxide, e.g. TiO_2,[14,15] *in situ* during spin coating. This approach surmounts a much encountered problem associated with the application of nanoparticles, which is that a common solvent for the polymer and the inorganic acceptor is required. Furthermore, as with polymer-nanoparticle systems, the high electron mobility of the inorganic phase can be utilized in favor of the photoinduced current.

Unfortunately, however, in polymer:TiO_2 solar cells from a molecular precursor the ill-defined structure of the metal oxide phase actually limits the current and thus the overall performance. At room temperature the titanium(IV) isopropoxide precursor is converted in air into amorphous TiO_2, whereas crystallization of the metal oxide would require incompatibly high temperatures well above 350 °C.[16] To overcome this limitation, Beek et al. have successfully made MDMO-PPV:ZnO solar cells with diethylzinc as a precursor for ZnO. Since ZnO crystallizes already at room temperature, moderate annealing temperatures can be used that are compatible with the presence of the conjugated polymer in order to prepare a well-performing inorganic semiconductor phase. From EQE measurements, promising power conversion efficiencies of 1.1% (AM1.5G, 1 kW/m^2) were estimated.[17]

In this chapter, we show that the chemical reaction of diethylzinc with moisture that takes place *in situ* during the fabrication of hybrid solar cells with MDMO-PPV has profound effects on the optoelectronic properties of the polymer. It is found that the polymer partially degrades, which has adverse effects on hole transport. Due to the chemical reaction, the photovoltaic behavior of these cells is unpredictable and their efficiency is rather low. To solve this problem, we demonstrate solar cells based on diethylzinc and P3HT, which is not affected by the chemical reaction during processing.

4.2 MDMO-PPV:ZnO solar cells using diethylzinc as precursor

The conversion of diethylzinc into ZnO is initiated upon exposure to water. Although the rate of the process is tempered by the addition of THF to the diethylzinc solution, it is

important to keep the humidity of the surrounding atmosphere at a constant level. In spite of the high level of control of the relative humidity in our experiments, we measured large variations in the performance of MDMO-PPV:ZnO solar cells with 15 vol % ZnO and a layer thickness of 100 ± 5 nm. Under illumination from a UV-filtered tungsten-halogen lamp with an intensity of approximately 0.8 sun, the most efficient cell gave a short-circuit current density J_{sc} of 20 A/m^2, an open-circuit voltage V_{oc} of 1.03 V and a fill factor FF of 0.41. An identical device processed on another day, however, showed a substantially reduced performance: $J_{sc} = 8.3$ A/m^2, $V_{oc} = 1.00$ V, and FF = 0.34. The parameters of another 40 devices were scattered randomly between these two extremes, which resulted in a substantially lower average efficiency of approximately 0.7%.

Because of this large variation in performance, an undesirable chemical side reaction is anticipated that has a detrimental effect on the structural and electronic properties of the polymer. The predominant degradation mechanism of conjugated polymers is photo-oxidation,[18,19] which generally leads to a deterioration of the photoconductivity and thus device performance under illumination in the presence of oxygen.[20] In poly(*p*-phenylene vinylene) (PPV) derivatives this degradation presumably results in a decrease of the conjugation length of the backbone. As the vinylene moiety is the most reactive part of the backbone, it is expected that the effects of the chemical reaction that is deliberately induced during spin coating involves polymer degradation through the breaking of trans vinyl (–C=C–) bonds.

Absorption spectroscopy

In Figure 4.1, the absorption spectrum of three different solutions of MDMO-PPV in chlorobenzene are shown. The solid line shows the absorbance of pristine MDMO-PPV dissolved directly after it was taken out of the stock bottle, whereas the dashed line represents the polymer after redissolving it from a pure MDMO-PPV layer that was spin coated on top of a glass substrate and subsequently aged and annealed in humid nitrogen. No effect on the absorption spectrum due to the processing under these conditions can be seen. However, a blueshift ($\Delta\lambda$) of 17 nm is found for the absorbance maximum of the polymer redissolved from a layer that was spin coated from a mixture of MDMO-PPV and diethylzinc under humid conditions (dotted line). Such a blueshift is indicative of a reduction of the conjugation length of the polymer. Clearly, it is reasonable to expect that at least a small amount of the trans vinyl bonds are affected during the chemical process of precursor conversion.

^{1}H NMR measurements

A change in chemical composition of the polymer should become apparent in proton nuclear magnetic resonance (^{1}H NMR) measurements. Since ^{1}H NMR spectra of poly-

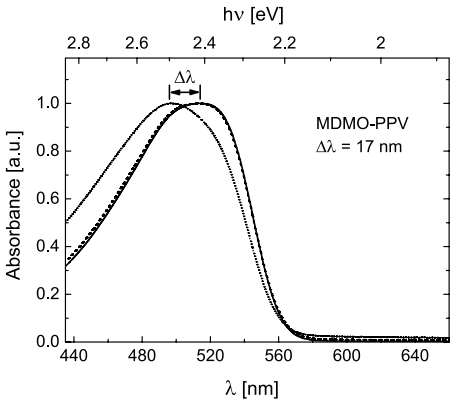

Figure 4.1: Absorption spectra of MDMO-PPV in chlorobenzene, dissolved directly from the stock bottle (solid line), redissolved from a processed layer of the neat polymer (dashed line), and redissolved from a composite layer with precursor ZnO (dotted line).

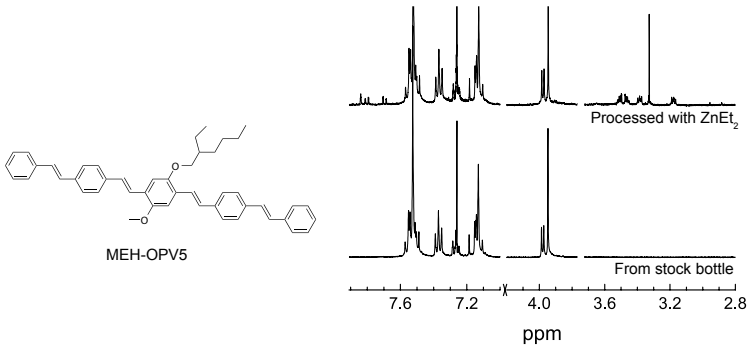

Figure 4.2: *Left:* Chemical structure of MEH-OPV5. *Right:* ^{1}H NMR spectra of MEH-OPV5 in $CDCl_3$, dissolved directly from the stock bottle (bottom) and redissolved from an MEH-OPV5:ZnO layer processed using *in situ* conversion of diethylzinc (top).

mers usually result in broad and ill-defined resonance peaks, we mimicked the processing using the model compound (*E*,*E*,*E*,*E*)-1,4-bis[(4-styryl)styryl]-2-methoxy-5-(2-ethylhexyloxy)benzene (MEH-OPV5, see Figure 4.2),[21] which was processed under similar conditions as the MDMO-PPV cells using diethylzinc. The pristine five-ring oligomer MEH-OPV5 contains four olefinic vinyl moieties that are clearly resolved by ^{1}H NMR. When diethylzinc (in a toluene/THF mixture) is introduced during the processing procedure, new peaks appear between 7.84 and 7.69 ppm. Furthermore, several ill-defined multiplets arise between 3.53 and 2.41 ppm. These additional shifts are reconcilable with disappearance of some of the vinyl bonds and the formation of oxidized species such as alcohol or ketone and the complementary formation of saturated C—C bonds. The most pronounced signs of degradation, however, were found in the deterioration of charge carrier transport.

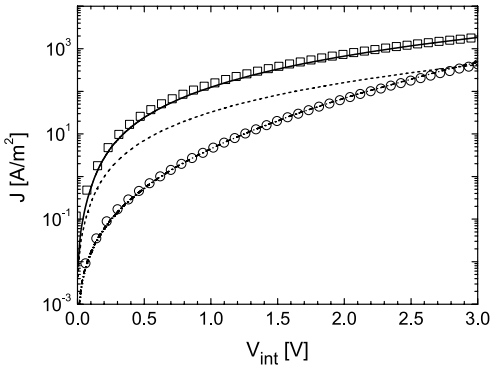

Figure 4.3: $J - V$ characteristics of hole-only devices based on MDMO-PPV (squares) and MDMO-PPV:ZnO (circles). The solid line represents a numerical fit using the single-carrier space-charge-limited current with a density-dependent mobility. The dashed line shows the calculated $J - V$ curve for the 95 nm thick MDMO-PPV:ZnO device, using the model parameters from the fit of the pristine MDMO-PPV diode ($L = 66$ nm). The dash-dotted line denotes a numerical simulation which takes into account a low mobility and a large field-activation parameter.

Hole mobility in an MDMO-PPV diode processed under humid conditions

Figure 4.3 shows the current densities under forward bias of hole-only devices from a neat MDMO-PPV layer (squares) and from a composite layer, in which ZnO is introduced via the conversion of diethylzinc (circles). Both layers were spin coated, aged and annealed in 40% relative humidity. The applied voltage was corrected for the built-in voltage (the voltage for which J becomes proportional to V^2) and the voltage drop over the series resistance of the ITO/PEDOT:PSS electrode (typically between 25 and 40 $\Omega/\square$) to obtain the internal voltage (V_{int}) over the active layer. We used our numerical device model,[22] assuming a density-dependent mobility, to make a fit to the hole-only current through the pristine MDMO-PPV device. This resulted in a zero-field hole mobility $\mu_h(0) = 5 \times 10^{-10}$ m^2/Vs, a conductivity prefactor $\sigma_0 = 3.1 \times 10^7$ S/m, an effective overlap parameter $\alpha^{-1} = 0.14$ nm and a width of the exponential density of states $T_0 = 518$ K. Since these values are common for MDMO-PPV at room temperature,[23] it is concluded that processing and annealing under humid conditions has no influence on hole transport in a pristine MDMO-PPV layer. Please note that the zero-field hole mobility of this batch of MDMO-PPV, which was synthesized via the sulfinyl route, is ten times higher than previously reported for MDMO-PPV.[24]

Hole mobility in an MDMO-PPV:ZnO diode processed with diethylzinc

In a bulk heterojunction of MDMO-PPV and ZnO from diethylzinc, the hole current density at low voltages is about two orders of magnitude lower than in the pristine polymer

layer and the slope of J versus V is much larger. This can be seen more clearly by comparison of the measured data of the 95 nm thick hybrid device with the calculated current–voltage characteristics. In the simulation, the model parameters of the pristine MDMO-PPV layer were used and only the layer thickness and dielectric constant were changed accordingly. Since the strong bias dependence of J could not be recovered in the simulation, a fit to the data of the hybrid layer could not made under the assumption of a purely density-dependent mobility. As an alternative indication of the change in hole transport, the data was fitted numerically using SCL currents with a high field-activation parameter of the mobility and a low zero-field hole mobility. The resulting room-temperature mobility $\mu_b(0) = 1.8 \times 10^{-12}$ m^2/Vs was more than two orders of magnitude lower than $\mu_b(0)$ in pristine MDMO-PPV and the field-activation parameter amounted to $\gamma = 1.3 \times 10^{-3}$ (m/V)$^{0.5}$. Such a value of γ is abnormally high for a conjugated polymer, which makes justification of this interpretation difficult. It nevertheless confirms that processing MDMO-PPV together with diethylzinc in a humid environment has a huge undesired influence on hole transport through the polymer, which can be caused by the disappearance of only a few percent of the vinyl double bonds.

We note that the incorporation of neutral traps for charge carriers in the polymer phase can also result in low currents and a strong dependency on voltage. However, using the numerical device model with neutral traps that are exponentially distributed in energy, there was no combination of parameters that could simultaneously describe the temperature dependence of the hole current and its variation with sample thickness consistently. For a given set of parameters extracted from fits to the temperature-dependent $J - V$ curves, the resulting calculated thickness scaling (see Ref. 25) of J was much stronger than the measured thickness dependence of the current density in multiple samples. Doubling the layer thickness resulted in a calculated current density that was an order of magnitude lower than the measured current, i.e., the dissimilarity was not caused by the uncertainty in the thickness measurements. Moreover, it was necessary to incorporate an additional field dependence of the mobility to obtain a good fit to the data. Therefore, neutral-trap-limited hole currents are inadequate in describing the observed effect.

The remarkable change in the hole-only device characteristics possibly arises from field-assisted detrapping of holes in the polymer, in which charged traps might have been introduced due to interactions with diethylzinc or its reaction products during processing of the layers. In this case the conductivity of the sample is increased as the escape rate of charges from an oppositely charged trap is enhanced by the presence of an applied electric field E (Frenkel-Poole emission, see Figure 4.4a).[26] The field dependence of the current density in this regime is given by:[27]

$$J \propto E \exp\left(\frac{\gamma_{\mathrm{FP}}\sqrt{E}}{kT}\right) \tag{4.1}$$

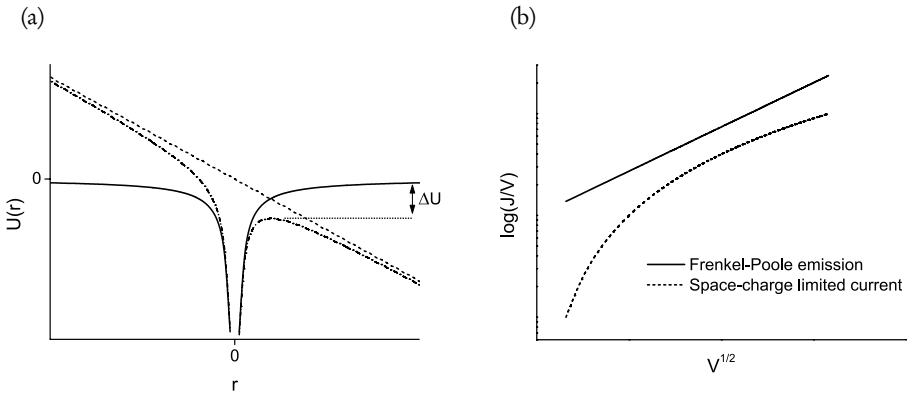

Figure 4.4: (a) Schematic representation of Frenkel-Poole emission. The Coulomb potential barrier (solid line) is lowered (dash-dotted line) by an amount ΔU in the direction of an applied electric field (dashed line). (b) A plot of $\log(J/V)$ versus $\sqrt{V}$ will result in a straight line when the current is dominated by Frenkel-Poole emission. This is not the case for space-charge-limited conduction.

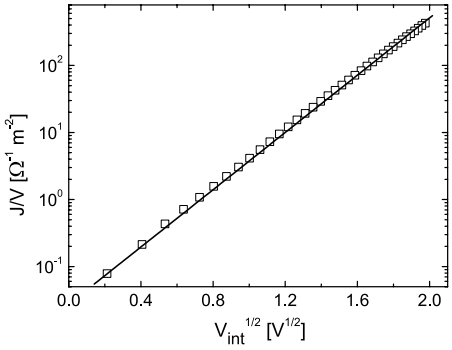

Figure 4.5: Plot of $\log(J/V)$ versus $\sqrt{V}$ for a 95 nm thick MDMO-PPV:ZnO hole-only device at room temperature. The solid line is a linear fit to the data.

with $\gamma_{\mathrm{FP}} = \sqrt{q^3/\pi\varepsilon}$. Under the assumption that the electric field can be approximated by $E \approx V/L$, a data plot of $\log(J/V)$ versus $\sqrt{V}$ should yield a straight line, in contrast to the case of SCL conduction (see Figure 4.4b).

In Figure 4.5, the current-voltage characteristics of the 95 nm thick MDMO-PPV:ZnO device are shown in the $\log(J/V)$ versus $\sqrt{V}$ representation. The data clearly follow a straight line, which indicates that the functional dependence of J on E as represented by Equation (4.1) can be used to interpret the data.

Using Eq. (4.1), we can fit the $J-V$ characteristics of our hybrid MDMO-PPV:ZnO hole-only diodes for various temperatures and thicknesses by allowing the field activation

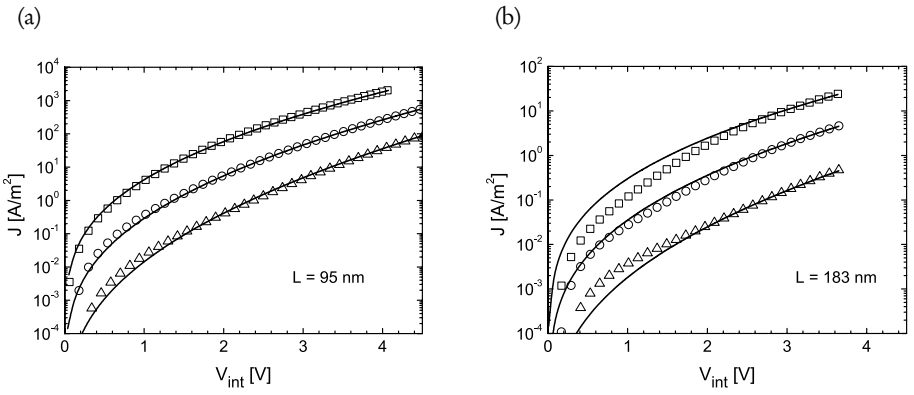

Figure 4.6: Current-voltage characteristics of MDMO-PPV:ZnO hole-only diodes with a thickness of (a) $L = 95$ nm and (b) $L = 183$ nm at $T = 295$ K (squares), $T = 255$ K (circles) and $T = 215$ K (triangles), using $\gamma/\gamma_{FP} = 0.85$. The lines are fits using Eq. (4.1).

parameter γ to vary. All fits shown in Figure 4.6 were made using $\gamma/\gamma_{FP} = 0.85$. From the fact that the field dependence of our data closely resembles that of Frenkel-Poole emission, we conclude that it is very likely that the deteriorated hole transport properties in MDMO-PPV:ZnO diodes is related to the introduction of charged traps due to the presence of diethylzinc.

In MDMO-PPV:PCBM cells, the hole mobility is enhanced due to the presence of the acceptor phase.[28] Hole conduction in cells from MDMO-PPV and ZnO nanoparticles shows no changes with respect to transport in the pristine polymer.[6] Therefore, the deterioration of hole transport through MDMO-PPV processed under humid conditions and in the presence of diethylzinc forms a major drawback in the use of this polymer for hybrid solar cells with precursor ZnO.

4.3 P3HT:ZnO solar cells using diethylzinc as precursor

Obviously, using a chemically more stable conjugated polymer is the most direct way of avoiding the processing-related deterioration of hole transport. Polythiophene derivatives, for example, do not contain vinyl moieties and are more resistant to oxidation than PPVs under identical circumstances.[29] By comparison of the absorbance, $J - V$ characteristics and fitted hole mobilities of P3HT with and without ZnO to the results on MDMO-PPV, we can conclude that P3HT is remarkably suitable for this purpose. Figure 4.7a clearly shows that the absorbance of P3HT in chlorobenzene is not influenced by first processing it under humid conditions, either in the presence of diethylzinc or without it. Also, as expected, the $J - V$ curves of hole-only devices from P3HT and P3HT:ZnO layers had similar slopes (Figure 4.7b). The difference in magnitude of J is due to a difference in layer

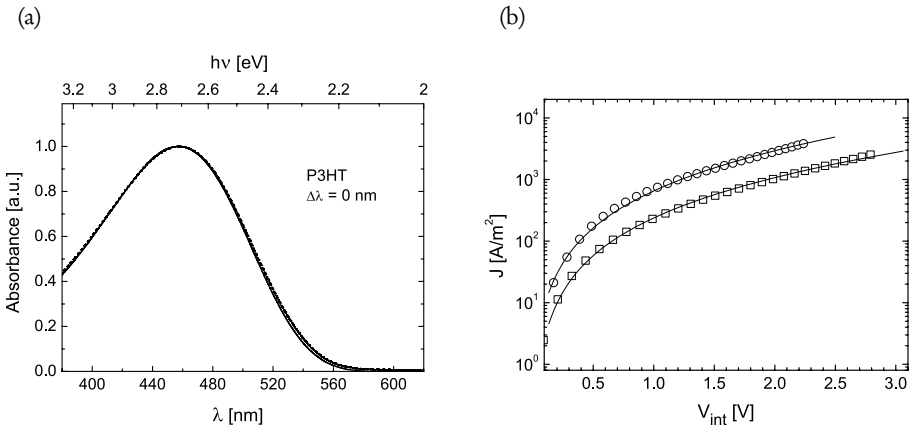

Figure 4.7: (a) Absorption spectra of P3HT in chlorobenzene, dissolved directly from the stock bottle (solid line), redissolved from a processed layer of the neat polymer (dashed line), and redissolved from a composite layer with precursor ZnO (dotted line). (b) $J-V$ characteristics of hole-only diodes made of P3HT (squares, $L = 141$ nm) and P3HT:ZnO (circles, $L = 117$ nm). The lines denote numerical fits with a density-dependent mobility.

thickness. The fitted density-dependent hole mobility at room temperature as determined with numerical simulations was equal for P3HT:ZnO and neat P3HT layers that were spin coated, aged and annealed in nitrogen with 40% relative humidity. The fits resulted in $\mu_h(0) = 2.0 \times 10^{-4}$ m^2/Vs, $\sigma_0 = 1.6 \times 10^6$ S/m, $\alpha^{-1} = 0.16$ nm and $T_0 = 425$ K, being equal to earlier reported values for pristine P3HT layers.[30] These results indicate that it might be advantageous to use P3HT instead of MDMO-PPV in BHJ solar cells with precursor ZnO.

Photovoltaic properties

To obtain a one-to-one comparison, we prepared photovoltaic devices from P3HT:ZnO with 15 vol % ZnO using the same procedure as for the cells from MDMO-PPV. The cells were characterized by IPCE and $J-V$ measurements at the Energy research Centre of the Netherlands (ECN), under illumination from a UV-filtered tungsten-halogen lamp setup with an intensity of circa 1.0 sun. A cell with a layer thickness of 102 nm resulted in a J_{sc} of 35 A/m^2, a V_{oc} of 0.83 V, and a FF of 0.50. This is illustrated in Figure 4.8, together with the $J-V$ curve of the most efficient MDMO-PPV:ZnO device of 96 nm thickness, measured at 0.8 sun intensity at the University of Groningen.

To account for the spectral mismatch, an estimation for J_{sc} of the P3HT:ZnO device under standardized AM1.5G, 1 kW/m^2 illumination ($J_{sc,calc}$) was made from the IPCE spectrum (see Figure 4.9). This was done by calculation of the spectral response from the IPCE data and integration of its product with the AM1.5G spectrum over the wavelength range

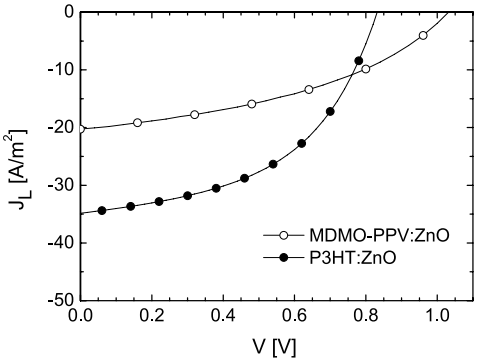

Figure 4.8: Comparison of the photovoltaic effect in MDMO-PPV:ZnO (open circles) and P3HT:ZnO (filled circles) diodes with 15 vol % ZnO, made via the precursor route using diethylzinc. The light intensity was 0.8 sun for the PPV-based cell and 1.0 sun for the P3HT:ZnO device.

from 380 to 950 nm, after making sure that the short-circuit current was linearly dependent on light intensity. The resulting calculated short-circuit current density amounted to 33 A/m^2, which is a factor of 1.4 higher than the $J_{sc,calc}$ previously reported for MDMO-PPV:ZnO cells.[17] It was then used together with the V_{oc} and FF from the $J-V$ measurements to obtain an estimated value of the AM1.5G power conversion efficiency η of 1.4%.

The improvement of the photovoltaic performance is mainly due to the large increase in J_{sc}. Unfortunately, this positive effect is opposed by a decrease in V_{oc} of 0.2 V. It is unlikely that this loss can be reduced, since the open-circuit voltage is a bulk property. For BHJ cells with ohmic contacts, V_{oc} is governed by the energy difference between the highest occupied molecular orbital (HOMO) of the donor and the lowest unoccupied molecular orbital (LUMO)[31] or, in this case, the conduction band edge (CBE) of the acceptor. Because the HOMO level of regioregular P3HT ($\approx$ 4.9 eV) is several tenths of an electronvolt closer to the CBE of ZnO than the HOMO level of MDMO-PPV ($\approx$ 5.2 eV), the observed reduction in V_{oc} is, most likely, inevitable.

Towards an improved efficiency of P3HT:ZnO cells

To further explore the potential of P3HT for solar cells with precursor ZnO, we fabricated devices with a ZnO content of 25 vol % and a layer thickness of about 200 nm. Assuming that the hole mobility in P3HT remains as high as before and that the percolation of the acceptor phase in the polymer matrix is enhanced by the increased amount of ZnO in the blend, one expects higher currents and thus an improved efficiency. Figure 4.9 demonstrates, however, that the IPCE spectra of the 25 vol % ZnO and 15 vol % ZnO

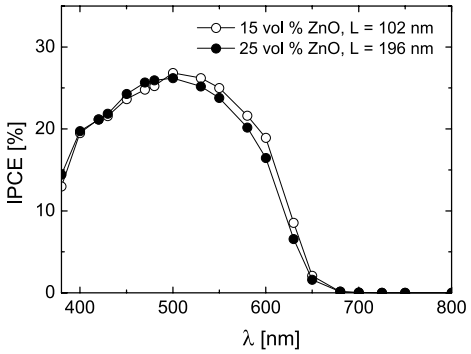

Figure 4.9: IPCE spectra of P3HT:ZnO solar cell with a ZnO content of 15 vol % (open circles) and 25 vol % (filled circles).

cells have similar shapes and maxima of approximately 26% at 500 nm. The calculation of the AM1.5G current for a 25 vol % ZnO cell gave a $J_{sc,calc}$ of 32 A/m^2, which, combined with a measured V_{oc} of 0.73 V and FF of 0.47, resulted in an estimated AM1.5G power conversion efficiency (PCE) of 1.1%. This efficiency is somewhat lower than in the P3HT photovoltaic cells with 15 vol% ZnO. From additional $J-V$ measurements on layers with a thickness up to 250 nm, however, we expect that the optimal thickness for the 25 vol % ZnO system is to be found beyond the 200 nm presented here. Further optimization of the hybrid polymer:ZnO system is needed in order to verify this.*

In agreement with the results of Beek and co-workers,[17] all precursor-route solar cells were found to withstand short-term UV illumination from a tungsten-halogen lamp without a significant decrease in performance. The shelf lifetime in nitrogen of unencapsulated P3HT:ZnO cells with 15 vol % ZnO was found to be limited due to a decrease of approximately 30% in both V_{oc} and FF after 46 hours of storage, reducing the maximum power point to about half its initial value. A proportional reduction was found by comparing η as measured at ECN in a solar simulator with a mismatch factor of 0.99, one day after processing, to the efficiency estimated with $J_{sc,calc}$ from the spectral response, which was measured shortly after processing. Strikingly, the short-circuit current was still at 80% of its initial value after one week.

4.4 Conclusions

In conclusion, we have shown by means of UV-VIS spectroscopy, ^{1}H NMR and charge carrier transport studies that the presence of highly reactive diethylzinc during the pro-

* During the realization of this thesis, the P3HT:precursor-ZnO system was investigated further by Oosterhout et al. They achieved a power conversion efficiency of 2% at a layer thickness of 225 nm and a ZnO volume fraction of 20 vol %.[32]

cessing of bulk heterojunctions of MDMO-PPV and ZnO causes the polymer to degrade. The degradation most likely involves a chemical reaction with trans vinyl bonds in the PPV backbone, and the conversion to a non-conjugated species. Therefore, we have prepared photovoltaic devices of precursor ZnO and P3HT, which does not contain trans vinyl groups. No influence of the processing on the UV-VIS absorption spectrum and hole transport properties of P3HT was found, indicating that diethylzinc does not affect this polymer. Without optimization, solar cells based on regioregular P3HT and precursor ZnO had an estimated AM1.5G power conversion efficiency of 1.4% and hence currently belong to the best performing polymer:metal oxide photovoltaic devices.

4.5 Experimental

Materials. MDMO-PPV ($M_w = 5 \times 10^5$ g/mol, PDI ~ 2.7, synthesized via the sulfinyl route) was obtained from TNO and used as received. Regioregular poly(3-hexylthiophene) (RR-P3HT, electronic grade; 98.5% regioregular; Rieke Metals, Inc.) was dissolved in distilled toluene, dedoped with hydrazine at 60 °C and precipitated in methanol. The fraction collected was Soxhlet extracted for at least 64 hrs with methanol, *n*-hexane, CH_2Cl_2 and finally with $CHCl_3$. The chloroform fraction was precipitated in methanol, dried under vacuum and stored in the glovebox under N_2 atmosphere. Properties of purified RR-P3HT: $T_g = 130$ °C, $M_w = 5 \times 10^5$ g/mol, PDI ~ 2. The structures of the polymers are shown in Figure 1.7(a).

Device fabrication. The preparation procedure of a typical solar cell based on a bulk heterojunction of MDMO-PPV and precursor zinc oxide is described below. The fabrication of samples based on regioregular P3HT was done analogously. A hole-transporting buffer layer of PEDOT:PSS was spin coated on top of a UV-ozone-cleaned glass substrate, patterned with indium tin oxide (ITO). The photoactive layer was spin coated from a mixed solution of MDMO-PPV and diethylzinc. This solution was prepared by the addition of the appropriate amount of a 0.4 M solution of diethylzinc in toluene and tetrahydrofuran (THF) to a solution of MDMO-PPV in chlorobenzene to give an overall polymer concentration of 5 mg/mL. Full conversion of diethylzinc into ZnO was assumed, which resulted in a volume fraction of 15 vol % ZnO in the heterojunction if a 1:1 weight ratio of the polymer and ZnO equivalent in the solution was used. The mixed solution (with a typical toluene to THF volume ratio of 1:2) was spin coated in nitrogen atmosphere with a relative humidity of 40%, controlled by the nitrogen flow through a gas diffusion bubbler. Subsequently, the hybrid film was aged for 15 minutes and annealed for 30 minutes at 110 °C in the same environment. The back contacts, consisting of 1 nm lithium fluoride (LiF) or 5 nm samarium (Sm) topped with 100 nm aluminum (Al), were thermally deposited in vacuum (10^{-6} mbar).

Hole-only diodes were constructed for hole transport studies by applying an electron blocking contact, consisting of 20–30 nm Pd and 60 nm Au, instead of the LiF/Al cathode. Under forward bias, the ITO/PEDOT:PSS bottom electrode served as an ohmic hole injection contact.

Characterization. The $J - V$ characteristics were recorded with a Keithley 2400 SourceMeter in nitrogen atmosphere, both in the dark and under illumination. The light source was a 50 W white light tungsten-halogen lamp. Because of the photocatalytic activity of ZnO (3.2 eV direct gap) that leads to the degradation of organic compounds in the UV region, [33] the lamp output was filtered with a Schott GG435 low-cut filter. The lamp/filter combination had a spectral range from 425 nm to 900 nm, with the maximum at 630 nm. The light intensity at the sample surface, i.e., after the UV filter, was approximately 0.8 kW/m^2 for MDMO-PPV:ZnO cells. P3HT:ZnO solar cells were characterized at ECN, The Netherlands, using a tungsten-halogen setup with an equivalent intensity of 1 kW/m^2. Transmittance and absorbance measurements on polymer solutions in quartz cuvettes were performed with a Perkin-Elmer Lambda 900 Spectrometer.

References

[1] G. Yu, J. Gao, J. C. Hummelen, F. Wudl, and A. J. Heeger, Science **270**, 1789 (1995).

[2] S. C. Veenstra, W. J. H. Verhees, J. M. Kroon, M. M. Koetse, J. Sweelssen, J. J. A. M. Bastiaansen, H. F. M. Schoo, X. Yang, A. Alexeev, J. Loos, U. S. Schubert, and M. M. Wienk, Chem. Mater. **16**, 2503 (2004).

[3] M. M. Mandoc, W. Veurman, L. J. A. Koster, M. M. Koetse, J. Sweelssen, B. de Boer, and P. W. M. Blom, J. Appl. Phys. **101**, 104512 (2007).

[4] C. Y. Kwong, A. B. Djurišić, P. C. Chui, K. W. Cheng, and W. K. Chan, Chem. Phys. Lett. **384**, 372 (2004).

[5] W. J. E. Beek, M. M. Wienk, and R. A. J. Janssen, Adv. Mater. **16**, 1009 (2004).

[6] L. J. A. Koster, W. J. van Strien, W. J. E. Beek, and P. W. M. Blom, Adv. Funct. Mater. **17**, 1297 (2007).

[7] W. J. E. Beek, M. M. Wienk, and R. A. J. Janssen, Adv. Funct. Mater. **16**, 1112 (2006).

[8] P. Ravirajan, A. M. Peiró, M. K. Nazeeruddin, M. Graetzel, D. D. C. Bradley, J. R. Durrant, and J. Nelson, J. Phys. Chem. B **110**, 7635 (2006).

[9] W. U. Huynh, J. J. Dittmer, and A. P. Alivisatos, Science **295**, 2425 (2002).

[10] B. Q. Sun, E. Marx, and N. C. Greenham, Nano Lett. **3**, 961 (2003).

[11] B. Q. Sun, H. J. Snaith, A. S. Dhoot, S. Westenhoff, and N. C. Greenham, J. Appl. Phys. **97**, 014914 (2005).

[12] K. M. Coakley and M. D. McGehee, Appl. Phys. Lett. **83**, 3380 (2003).

[13] K. M. Coakley, Y. X. Liu, M. D. McGehee, K. L. Frindell, and G. D. Stucky, Adv. Funct. Mater. **13**, 301 (2003).

[14] P. A. van Hal, M. M. Wienk, J. M. Kroon, W. J. H. Verhees, L. H. Slooff, W. J. H. van Gennip, P. Jonkheijm, and R. A. J. Janssen, Adv. Mater. **15**, 118 (2003).

[15] L. H. Slooff, M. M. Wienk, and J. M. Kroon, Thin Solid Films **451-452**, 634 (2004).

[16] M. Okuya, K. Nakade, and S. Kaneko, Sol. Energy Mater. Sol. Cells **70**, 425 (2002).

[17] W. J. E. Beek, L. H. Slooff, M. M. Wienk, J. M. Kroon, and R. A. J. Janssen, Adv. Funct. Mater. **15**, 1703 (2005).

[18] R. D. Scurlock, B. J. Wang, P. R. Ogilby, J. R. Sheats, and R. L. Clough, J. Am. Chem. Soc. **117**, 10194 (1995).

[19] G. H. Gelinck and J. M. Warman, Chem. Phys. Lett. **277**, 361 (1997).

[20] H. Neugebauer, C. J. Brabec, J. C. Hummelen, and N. S. Sariciftci, Sol. Energy Mater. Sol. Cells **61**, 35 (2000).

[21] V. V. Krasnikov, C. Melzer, L. Ouali, B. de Boer, U. Stalmach, and G. Hadziioannou, Polym. Prepr. **41**, 857 (2000).

[22] L. J. A. Koster, E. C. P. Smits, V. D. Mihailetchi, and P. W. M. Blom, Phys. Rev. B **72**, 085205 (2005).

[23] C. Tanase, P. W. M. Blom, and D. M. de Leeuw, Phys. Rev. B **70**, 193202 (2004).

[24] P. W. M. Blom, M. J. M. de Jong, and J. J. M. Vleggaar, Appl. Phys. Lett. **68**, 3308 (1996).

[25] K. C. Kao and W. Hwang, *Electrical Transport in Solids*, Pergamon Press, Oxford, 1981.

[26] J. Frenkel, Phys. Rev. **54**, 647 (1938).

[27] S. M. Sze, *Physics of Semiconductor Devices*, Wiley Interscience, 1981.

[28] C. Melzer, E. J. Koop, V. D. Mihailetchi, and P. W. M. Blom, Adv. Funct. Mater. **14**, 865 (2004).
[29] B. H. Cumpston and K. F. Jensen, Synth. Met. **73**, 195 (1995).
[30] C. Tanase, E. J. Meijer, P. W. M. Blom, and D. M. de Leeuw, Phys. Rev. Lett. **91**, 216601 (2003).
[31] V. D. Mihailetchi, P. W. M. Blom, J. C. Hummelen, and M. T. Rispens, J. Appl. Phys. **94**, 6849 (2003).
[32] S. D. Oosterhout, M. M. Wienk, S. S. van Bavel, R. Thiedmann, L. J. A. Koster, J. Gilot, J. Loos, V. Schmidt, and R. A. J. Janssen, Nat. Mater. **8**, 818 (2009).
[33] M. R. Hoffmann, S. T. Martin, W. Y. Choi, and D. W. Bahnemann, Chem. Rev. **95**, 69 (1995).